applied sciences

MDPI

Article

Bi-Functionalized Clay Nanotubes for Anti-Cancer Therapy

William R. Grimes [1], Yangyang Luo [1], Antwine W. McFarland Jr. [1] and David K. Mills [2,3,*]

[1] Molecular Sciences and Nanotechnology Program, Louisiana Tech University, Ruston, LA 71272, USA; rgrimes22311@gmail.com (W.R.G.); yangyang317luo@gmail.com (Y.L.); awm011@latech.edu (A.W.M.J.)
[2] Center for Biomedical Engineering and Rehabilitation Science, Louisiana Tech University, Ruston, LA 71272, USA
[3] School of Biological Sciences, Louisiana Tech University, Ruston, LA 71272, USA
* Correspondence: dkmills@latech.edu; Tel.: +1-318-267-5644; Fax: +1-318-257-4574

Received: 7 December 2017; Accepted: 8 February 2018; Published: 13 February 2018

Featured Application: Functionalized Halloysite Nanotubes for Targeted Drug Delivery.

Abstract: Systemic toxicity is an undesired consequence of the majority of chemotherapeutic drugs. Multifunctional nanoparticles with combined diagnostic and therapeutic functions show great promise towards personalized nanomedicine. Halloysite clay nanotubes (HNTs) have shown potential as a drug delivery vehicle, and its surface can be modified and tailored as a targeted drug delivery system. In this short report, we modified the HNT surface by covalently bonding folic acid (FA) and fluorescein isothiocyanate (FITC). The modification of HNTs with folic acid imparts the potential to target tumor cells selectively. The addition of FITC offers a method for quantifying the effectiveness of the FA tagged HNTs ability to target tumor cells. We documented cell uptake of our bi-functionalized HNT (bHNT) through phase contrast and epi-fluorescent microscopy. bHNTs showed no signs of cytotoxicity up to a concentration of 150 μg/mL. The increase in cell death with increased bHNT concentration may be due to induced cytotoxicity resulting from intracellular bHNT accumulation that disrupts cellular function leading to cell death. With HNTs recognized as having the ability to serve as both a nanocontainer and nanocarrier, we envision our construct as a potential modular platform for potential use in cancer therapeutics. The HNT interior can be loaded with a variety of anti-cancer drugs (or other chemotherapeutics) and serve as a "death cargo" designed to kill cancer cells while providing feedback imaging data on drug efficacy. The surface of the HNT can be modified with gold or silver nanoparticles and used in photothermal therapy by converting light to heat inside tumors. Our HNT-based drug delivery system has the potential to provide localized and targeted therapies that limit or reduce side effects, reduce patient costs and length of hospital stays, and improve quality of life. However, further research is needed to validate the potential of this new chemotherapeutic drug delivery system.

Keywords: cancer therapy; drug delivery; folic acid; halloysite nanotubes; nanotechnology; surface functionalization

1. Introduction

For patients who are suffering from advanced or highly invasive cancer and have lost the opportunity for surgery, chemotherapy remains the best treatment option. One of the biggest limitations to current cancer therapeutics is their lack of a specific targeting mechanism that avoids nonspecific toxicity to healthy tissue [1]. Nanotechnology offers a unique opportunity for overcoming non-specific tissue targeting and the unwanted toxic side effects of current chemotherapeutics [2–4]. Of the nanopharmaceuticals currently on the market, very few are designed to treat cancer [5,6].

To decrease the toxic effects associated with paclitaxel, for example, a nanoparticle formulation for paclitaxel was introduced under the trade name Abraxane [5,6]. A reduction in toxicity was accomplished by binding paclitaxel with albumin in a protein-bound nanoparticle followed by nanoparticle dissolution and release of an albumin-bound drug complex [6–8]. While this system has been successful and has been on the market since 2005, its major drawback is that it lacks a targeting system [5,6]. This design limitation has led to intense research directed towards the fabrication of nanoparticles with surface ligands capable of targeting a specific tumor [9–11]. Furthermore, nanoparticles are being designed that not only deliver a drug to the tumor site but also have a tracking moiety bound to the surface of the nanoparticle itself [5]. With the combination of tracking and targeting moieties, it is expected that cancer treatments will lead to significantly improved patient outcomes [10,11].

Different types of nanoparticles designed for multi-functionality have been investigated. Some systems are capable of carrying two separate drugs in one nanocarrier [1,3,4,12]. Other nanocarrier systems are bi-functionalized so they are capable of targeting cancerous tissue and delivering a cancer drug [7,13]. Other nanocarriers contain a third functionality that enables real-time monitoring of the nanoparticle's movement through the body [14]. These systems are of particular interest because they permit monitoring of the effectiveness of the targeting system as well as drug release [2,9,11]. One nanocarrier that has potential to become a critical component of bi-functional nanoparticle systems are halloysite clay nanotubes (HNTs). HNTs are naturally occurring clay nanoparticles that have emerged as a potent nanocontainer and nanocarrier for drug delivery [15–17]. HNTs are formed through strain caused by lattice mismatch between the adjacent silicon dioxide and aluminum oxide layers [15–17]. HNTs have found numerous commercial applications as additives in polymers and plastics, electronics components, cosmetics and personal care products [17,18]. HNTs are unique and versatile nanomaterials that are composed of a double layer of aluminum, silicon, hydrogen, and oxygen [15–17]. HNTs are ultra-thin hollow tubes with diameters typically smaller than 100 nanometers, with lengths typically ranging from 500 nanometers to over 1.2 microns [15,19].

Due to the chemical makeup of the HNT lumen, it is capable of being doped with a diverse set of substances including antibiotics, chemotherapeutics, growth factors, RNA and DNA, and used as a vehicle for drug transportation and sustained release [20–23]. Additionally, several recent studies have demonstrated that HNTs are cytocompatible [20,24–26]. In one study, HNTs were added to cultures of epithelial adenocarcinoma and human breast cancer cells up to a concentration as high as 75 μg/mg) and cell proliferation was not affected [24]. In fact, most studies have shown that the HNTs do not produce cytotoxic effects [20,24–26]. Recently, Cervini-Silva et al. in 2012 showed that HNTs also have anti-inflammatory properties [27].

Research interest in the surface modification of HNTs has grown significantly in recent years [28]. The majority of these efforts have been directed towards improving HNT dispersion within a polymer, polymer/nanoclay composite compatibility, and functionalizing the HNT surface [28,29]. Joo et al. (2012), for example, modified hydroxyl groups on the HNT surface to carboxylic acids to show the potential of these hydroxyl groups [30]. The HNT surface has been successfully altered with a variety of organosilanes. Du et al. (2006) functionalized the HNT surface with γ-aminopropyltriethoxysilane and then polypropylene chains were grafted onto the HNT surface with a resultant increase in mechanical properties compared with polypropylene alone or polypropylene/unmodified HNTs [31]. HNTs were successfully modified with different functionalized organosilanes, and interestingly, the analysis indicated that HNT dispersion in poly(hydroxybutyrate-co-hydroxyvalerate) (PHBV) led to various structures depending on the clay organomodifier [32]. The authors concluded that the mechanical properties of HNT/PHBV composites could be altered with the final composition dependent on the clay organomodifier [32]. Furthermore, silane-functionalized HNTs have been developed for many

applications in polymer matrices, such as epoxy resin [33], polypropylene [31], natural rubber [34], and ethylene-propylene-diene rubber [35].

In contrast, the area of chemical modification of HNTs via covalent bonding for drug delivery applications is an area that has seen only a few studies using bioactive molecules [36]. In one study, modification of the inner surface using phosphonic acid was reported to produce an increase in drug loading capacity [24]. Another study used molecules grafted onto the surface to create sulfur bridges as a means of glutathione selectivity in addition to pH sensitivity demonstrating an efficient chemotherapeutic delivery system [37].

Here, we describe the synthesis of a bi-functionalized HNT with two different molecules covalently bound to the outer HNT surface. In contrast to healthy cells, tumor cells overexpress specific receptors and tumor-associated surface antigens [38]. Among these, the folate receptor (FR) is overexpressed by a wide range of tumors such as ovary, kidney, colon, breast, and lung cancers [39–41]. Folic acid (FA), an oxidized form of folate, can bind to the membrane-anchored FRs and increase cellular uptake, which makes it a specific ligand to target FR-overexpressing tumor cells. The addition of FA to the surface of the HNTs will allow for selective targeting of tumors [39,40]. Furthermore, the addition of fluorescein isothiocyanate (FITC) to the surface creates a method by which the effectiveness of the targeted system can be determined via in vivo imaging [16]. Additionally, this study describes a washing process for the HNTs, post modification, that is not reported in similar studies [24,33,37,42–45]. The resulting modified HNTs were characterized via FTIR, 13C{H1}CPMAS NMR, and UV-Vis spectroscopy. As a proof of concept, bi-functionalized HNTs (bHNTs) were assessed for cytotoxicity and evaluated for their ability to be internalized by murine colon cancer cells through fluorescent microscopy.

2. Materials and Methods

2.1. Materials

All cell culture reagents including a LIVE/DEAD™ Viability/Cytotoxicity Kit were purchased from ThermoFisher, Waltham, MA, USA. All glassware and reagents were purchased from Sigma Aldrich, St. Louis, MO, USA, and were used as is unless indicated below. Cell culture dishes, pipettes and other disposable plastics were purchased from Mid Sci., St. Louis, MO, USA, Murine colorectal cancer cells (CT26.WT, ATCC® CRL-2638™) were purchased from American Type Culture Collection (ATCC) Manassas, VA, USA.

2.2. Methods

2.2.1. HNT-DAS-FA/FITC Synthesis

Briefly, a three-neck flask affixed with a Dean-Stark trap, 8.0014 g HNTs was suspended in 200 mL toluene. To the suspension, 35 mL of N-[3-(trimethoxysilyl)propyl) ethylenediamine (DAS) was added and refluxed at 115 °C for 24 h. After the reaction was complete, the suspension was then removed, washed and filtered using methanol, sodium chloride solution, sodium bicarbonate solution, and distilled water (DI) water. Following the addition of the DAS, 5.0049 g of washed HNT-DAS was suspended in the minimum amount of DI water necessary. To this suspension, 4.5 mg of FA was added followed by the addition of 2.6 mg of 1-ethyl-3-(3-dimethylaminopropyl)carbodiimide (EDC) to the suspension. The reaction was stirred at room temperature overnight.

The resulting compound was washed in the same manner as the HNT-DAS. Following the synthesis of HNT-DAS-FA, a small portion was exposed to 3 M NaOH overnight and the resulting solution was filtered. After the conjugation of FA to the HNT-DAS, 2.4979 g of HNT-DAS-FA was removed and added to 0.0025 g of FITC in acetone. The suspension was allowed to stir overnight at room temperature. The resulting compound was washed and filtered in the same manner as previously described. Following the synthesis of HNT-DAS-FA/FITC, a small portion was reacted

with 3 M NaOH overnight to cleave the covalent bonds and release the FA and FITC from the surface of the HNTs. A schematic representation of the synthesis process is presented in Figure 1.

Briefly, HNTs were reacted at reflux with DAS in toluene for 24 h. The HNT-DAS was then reacted with FA in the presence of *N*-(3-dimethylaminopropyl)-*N′*-ethylcarbodiimide hydrochloride (EDC) in DI water overnight.

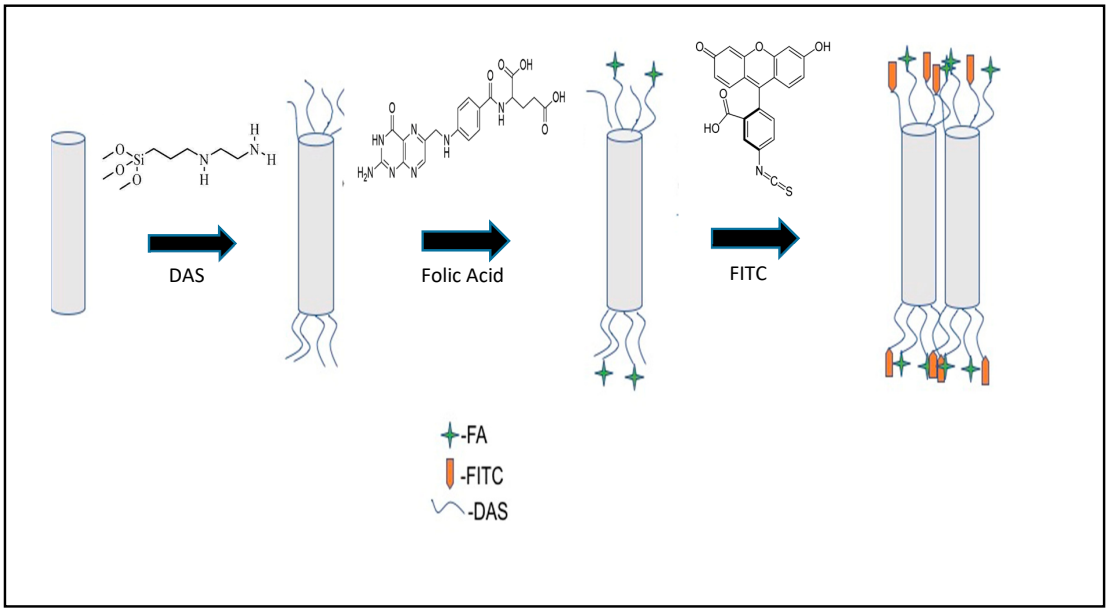

Figure 1. Schematic representation of the conjugation of both FA and FITC to DAS which is attached to the surface of the HNTs. DAS = *N*-[3-(trimethoxysilyl)propyl) ethylenediamine, FA = folic acid, FITC = fluorescein isothiocyanate.

Following the synthesis of HNT-DAS-FA, the complex was reacted with FITC in acetone overnight. After each synthetic step, the complex was washed and filtered. To wash the products, they were subsequently suspended in a sodium chloride solution, sodium bicarbonate solution, and methanol. This was followed by a wash using DI water.

2.2.2. HNT-DAS-FA/FITC Characterization

The nanoparticles were characterized via FTIR, 13C{H1}CPMAS, and UV-Vis. FTIR spectra were obtained using a Thermo Scientific (Waltham, MA, USA) IR100 and KBr IR spectra were acquired with a Mattson Genesis II FTIR. A Shimadzu 2401 UV-Vis spectrometer (Tokyo, Japan) operating with the UVProbe software package, supplied as standard with Shimadzu UV-VIS Spectrophotometers. The UVProbe software was used to identify the presence of FA and FITC in solution. Additionally, a Thermo-Fisher NanoDrop 2000 was used to acquire UV-Vis data. All UV-Vis samples were placed in standard 1 cm quartz cuvettes. Solution state ^{1}H NMR was obtained using a Bruker AVIII HD 500 MHz spectrometer (Bruker, Milton, ON, Canada) with a Prodigy probe. All experiments were done at ambient temperature (300 K). Spectra were obtained for the starting material (HNT), intermediates (HNT-DAS and HNT-DAS-FA), and final product (HNT-DAS-FA/FITC). The 13C{H1}CPMAS analyses were run at 4 kHz for 156,000 scans.

2.2.3. Cell Culture

Cytotoxicity of bi-functionalized (coated) HNTs were studied in CT-26 murine colorectal cancer cells. Murine colorectal cancer cells (CT-26) came cryopreserved from ATCC. Cryovials were thawed and allowed to equilibrate in a water bath within a humidified CO_2 incubator at 37 °C, 95% air and 5% CO_2. Cells were cultured in T25 culture flasks, maintained in Roswell Park Memorial Institute

(RPMI 1640 medium containing 10% FBS and 1% penicillin (complete medium) through passage four and then frozen down and maintained in a liquid nitrogen Dewar until use. A trypsin-EDTA (0.25% trypsin, 1 mM EDTA) was used to detach cells from the culture flasks.

For all experiments (n = 3), CT-26 cells were thawed as described above, plated in T25 culture flasks and maintained in RPMI 1640 medium until cultures were subconfluent. For cytotoxicity and uptake experiments, cells were enzymatically detached as described above, rinsed in complete medium, and centrifuged to collect the liberated cells. CT-26 cells (1×10^5 cells/96 well) were then resuspended in complete medium and cultured for 24 h. Then, the medium was removed and replaced by RPMI 1640 medium with bHNTs at concentrations of 25, 50, and 150 μg/mL. Cells cultured without NPs were used as control. All cultures were maintained for an additional 24 h before testing for potential cytotoxicity.

2.2.4. Live/Dead Cytotoxicity Assay

CT26 cells were cultures and exposed to bHNTs as described above. Cell viability after exposure to bHNTs was performed using a LIVE/DEAD® Viability/Cytotoxicity Kit (ThermoFisher). The kit contains the polyanionic dye calcein, which is retained within living cells and produces an intense uniform green fluorescence (ex/em ~495 nm/~515 nm) and EthD-1, which enters cells with damaged membranes and produces a bright red fluorescence in dead cells (ex/em ~495 nm/~635 nm). For viability studies staining solution was prepared by mixing 5 μL of 4 mM Calcein AM Solution and 20 μL of 2 mM EthD-III Solution to 10 mL of DPBS. Cell culture plates were washed twice with DBSS and then 100 μL of staining solution was added to each well plate. These substrates were then incubated at room temperature for 30 min. Each cytotoxicity experiment was repeated three times. Images were captured using an Olympus BX51 fluorescence microscope (Olympus Corporation, Tokyo, Japan) equipped with an Olympus DP11 digital camera system.

3. Results and Discussion

3.1. Fabrication and Analysis of the HNT-DAS-FA/FITC Complex

After each synthetic step, an FTIR spectrum was obtained from the product. Upon sample inspection, IR analysis showed peeks associated with the grafting of the molecule DAS on the HNTs outer surface, and this result agrees with reported spectra published in previous studies. 42–46 Peeks of interest included N-H_2 scissoring at 1556 cm^{-1}, Si-CH deformation at 1329 cm^{-1}, and the bending associated with NH at 1654 cm^{-1} as depicted in Figure 1 part b. Additionally, the 13C{H1}CPMAS showed aliphatic carbons associated with DAS and is illustrated in the supplemental information 2. The 13C{H1}CPMAS of unmodified HNTs is presented in supplemental information 1 for comparison.

Upon conformation that the DAS was successfully grafted to the HNT surface, FA was tethered to the primary amine of the DAS via amide bond formation (Figure 1). The signals normally associated with the primary amine of DAS were reduced, and the appearance of a noisy signal between 1500–1300 cm^{-1} was attributed to the attachment of FA to the DAS/HNT (Figure 2). In addition to the FTIR data, the 13C{H1}CPMAS spectrum showed the presence of carbonyl peeks as well as carbons associated with a conjugated ring. Additionally, after the HNT-DAS-FA was thoroughly washed to remove any unreacted material bound to the surface via weak interactions, a sample was exposed to 3 M NaOH to cleave the bonds tethering the FA to the surface of the HNTs. This reaction would release any compound chemically attached to the HNT surface remaining after the washing procedure. A solitary peek at 280.83 nm was observed in solution and is attributed to folic acid. Due to the reduction of the amine peaks, and the presence of only the folic acid after the wash phase, we conclude that folic acid had been successfully grafted to the DAS.

Following successful formation of the HNT-DAS-FA complex, a fluorescent tag (FITC) was then added to the remaining DAS molecules that were not reacted with the FA in the previous step. Analysis of the sample via FTIR did not show a change from the last IR obtained of HNT-DAS-FA.

However, upon decomposition of the samples with 3 M NaOH, both FA and FITC were present in the solution. It can be concluded that the FA was covalently bound to the DAS because it was not removed through washing or during the reaction with the FITC and subsequent washing process. Upon inspection of the 13C{H1}CPMAS of HNT-DAS-FA/FITC, little change was observed. This is not unexpected in that the carbons found in FITC are similar to those found in FA. Therefore, the peek positions would not change.

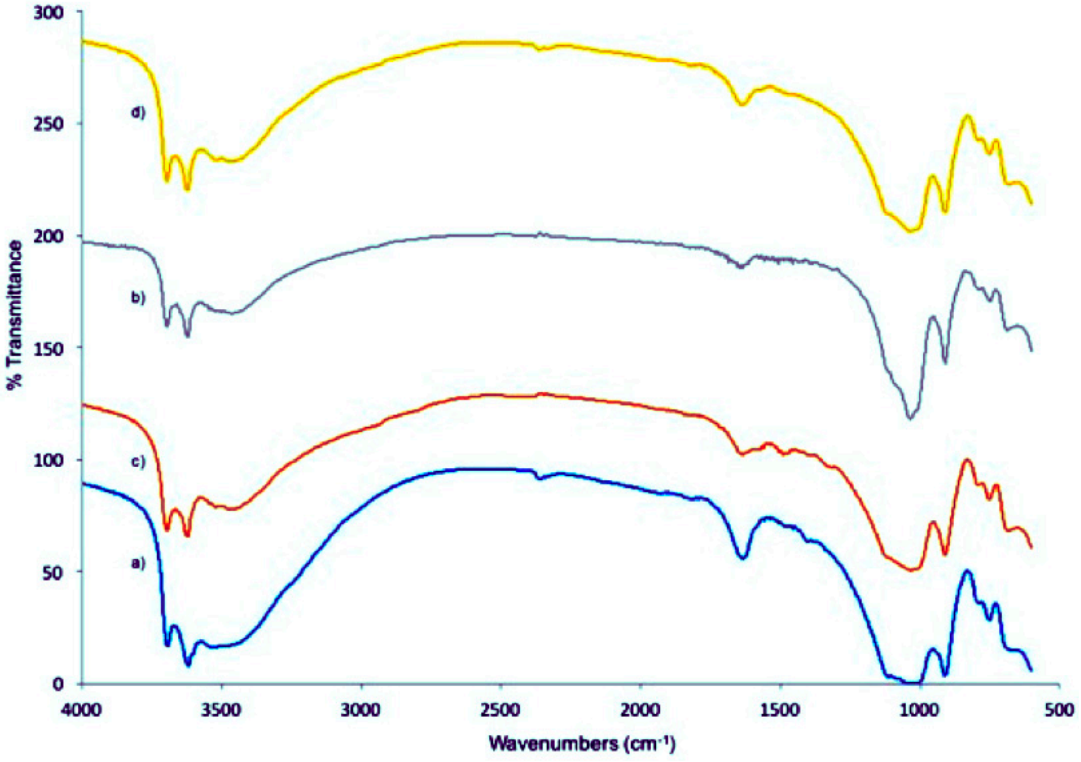

Figure 2. FTIR obtained of (**a**) HNT; (**b**) HNT-DAS; (**c**) HNT-DAS-FA; (**d**) HNT-DAS-FA/FITC.

The signals in both FTIR and 13C{H1}CPMAS were weak when compared to the spectra present in the literature [13]. However, when coupled with the FTIR data, our group concludes that the number of molecules capable of grafting to the surface of the HNTs is lower than that reported in other similar studies [42–45]. In previously reported studies, the solvents used for the reaction were used to wash the compounds after the synthesis [42–45]. While this would remove some excess material, this method is ineffective at removing the material bound to the surface of the HNTs that is deposited in layer-by-layer self-assembly [20,46,47]. This would lead to greater amounts of compounds being retained on the surface of the HNTs, and thus a larger signal for FTIR and NMR would result. The method for cleaning described would overcome this problem by removing any non-covalently bound compounds from the surface of the HNTs. Coupling the FTIR and NMR data the presence of the compounds post decomposition is evidence that the FITC and FA were covalently attached to the HNT surface (see Supplementary Materials data). Additionally, upon inspection of the ratio of FA to FITC fond in the decomposition of the final product, it was found to be approximately a 1:1 ratio that fits with our synthetic design.

3.2. Cellular Uptake of bHNTs

CT-26 cancer cells were exposed to unmodified HNTs at concentrations ranging from 50 to 150 μg/mL. When viewed under phase contrast or bright field light, CT-26 cells cellular morphology was unaffected (Figure 3A). Under the epifluorescent light, the brown accumulations within cells correspond to a similar concentration of bHNTs tagged with FITC (Figure 3A). When a

brightfield image in Figure 3A is compared with fluorescent images of the same field (Figure 3B), the correspondence between the green fluorescence areas and the brown accumulations is striking (Figure 3).

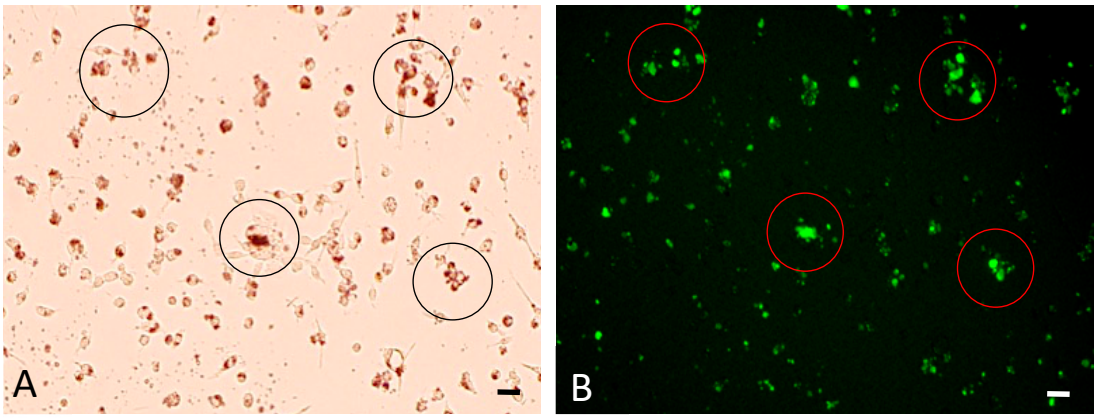

Figure 3. Cellular Uptake Assay (**A**) Phase contrast image of CT-26 cells after exposure to bHNTs (50 μg/mL). Brown intracellular accumulation indicates presence of bHNTs within the cell cytoplasm; (**B**) The same field of view (black circles in A) observed under epifluorescent light. Brown intracellular accumulation as seen in A correspond to FITC-tagged bHNTs in B showing up take by CT-26 cells.

3.3. Cytotoxicity Testing of bHNTs

Cytotoxicity of bHNTs was studied in CT-26 murine colorectal cancer cells at concentrations up to 150 μg/mL. Control cells cultured with unmodified HNTs at all concentrations showed no signs of cytotoxicity based on Live/Dead analyses (Figure 4). CT-26 cells cultured with bHNTS at concentrations up to 150 μg/mL also showed little evidence of cell death. When the same visual fields were observed with epifluorescence microscopy, live cell showed a green fluorescence while dead cells fluorescence a reddish orange (Figure 4). After 150 μg/mL, the number of dead cells observed increased with increased bHNT concentration. There are two possible explanations for this observation. Cell death may be due to induced cytotoxicity due to exposure to increased concentrations of bHNTs. However, numerous in vitro and in vivo studies have shown that HNTs are cytocompatible and biocompatible [48–52]. Sun et al. (2016) showed that osteosarcoma cells exposed to HNTs at a concentration of 2000 μg/mL suffered no cytotoxic effect after exposure [20]. An alternative explanation is that intracellular bHNTs accumulation disrupts cellular function. The cell interior is a crowded space and once inside the cells BHNTs may accumulate leading to cell death. Nanoparticle uptake and accumulation in cells can disrupt critical intracellular transport pathways and organellar functions as detailed in Panariti et al. (2012) [53].

Recently, Hu et al. (2017) used halloysite as a vehicle for developing an anti-cancer drug delivery system [54]. They described the synthesis of an HNT nanodelivery system modified with thiol groups, which served as a binding site for the B-cyclodextrin used to cap the ends of the HNTs. Disulfide bonds, which can be cleaved at both acidic and basic pH environments, were used to bind the B-cyclodextrin to the ends of the HNTs in order to entrap the doxorubicin (DOX) within the HNT lumen. Following this procedure, PEG conjugated with FA was deposited on the outer HNT surface. This HNT complexed DOX system accelerated the apoptosis of cancer cells as compared to non-targeted HNTs.

While their system does impart a dual functionality to the HNTs, it does differ from our HNT drug delivery system. First, the HNTs were capped using cyclodextrin and our system does not include a capping system but a means to entrap the cargo and regulate its release could be can be added [52,54,55]. Instead, the HNT-DAS-FA/FITC includes both an imaging and targeting agent covalently attached to the surface of the HNTs. By incorporating an imaging moiety in the system, the efficacy of the treatment option can be monitored. Additional, the HNT-DAS-FITC/FA is modular

and was designed to attach bioactive molecules that use amide bonds as well as similar bonding moieties, thus allowing the system to be applied to a range of cellular targets.

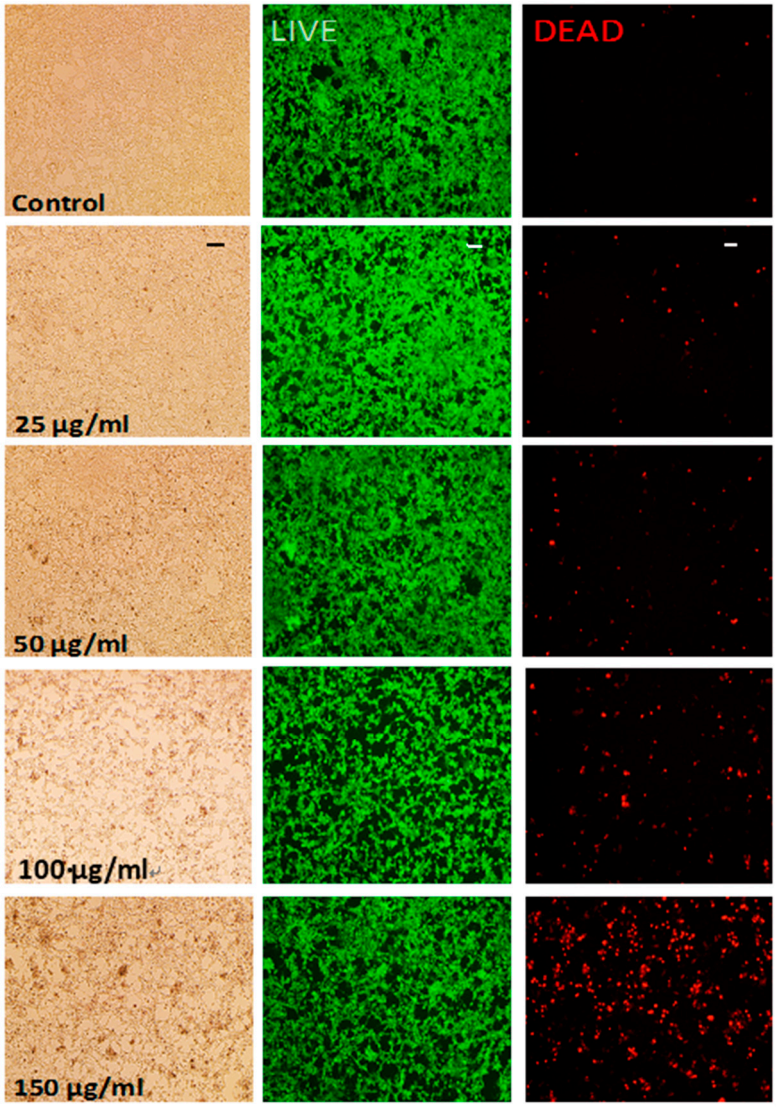

Figure 4. Live/Dead Assay. CT-26 cells were culture in the presence of bHNTs at 0, 25, 50, 100 and 150 µg/mL. From left to right, brightfield, green filter (live cells) and red filter (dead cell) images. Bar = 100 microns.

Secondly, the system proposed by the Hu group uses FA-conjugated to PEG deposited on the outer surface of the HNTs. Acidic and basic conditions are commonly used in the layer-by-layer surface coatings applied to devices to dissociate the bonds linking the various polyelectrolytes together [56]. Our system prevents the dissociation of FA from the surface by covalently linking it to the DAS. Furthermore, the lumen of HNTs makes them a particularly interesting nanocarrier for the loading and release of various biologically active molecules, including small molecules, enzymes, and proteins including chemotherapeutic payloads [54–61]. We envision our construct as a potential modular platform for use in anti-cancer therapies. The HNT interior can be doped with anti-cancer drugs (or other chemotherapeutics) and serve as a "death cargo" designed to kill cancer cells and provide imaging data on the drug's effects. The HNT surface can also be modified with gold, silver or iron nanoparticles. The metal-coated bHNTs could then be used in photothermal therapy by converting light to heat inside tumors. Iron-coated bHNTs aimed for anti-cancer therapies based on magnetic

hyperthermia is another possibility. Our bi-functionalized HNT drug delivery system can target cancer cells without injuring normal cells providing localized and targeted therapies that limit or reduce side effects, reduce patient costs and length of hospital stays, and improve the quality of life.

However, several questions regarding this anti-cancer nanoparticle remain to be answered and are the basis for current and future studies. Is the observed increase in cell death with exposure to concentrations greater than 150 μg/mL to a cytotoxic response or due to disruption of cell function? Do the bHNTs accumulate or are they degraded in the cell? Is their accumulation toxic to cells? What is the mechanism of cell death, necrosis or apoptosis? Furthermore, the mechanism by which bHNTs enter the cells has important implications not only for their ultimate fate but also for adding a "death cargo", a drug or additional surface modifications (i.e., gold nanoparticles) that will kill the tumor directly. At present, our continuing research efforts are directed towards testing the HNT-DAS-FA/FITC in osteosarcoma cell culture as a means of validating and assessing the utility of the system as a targeted drug delivery vehicle. Additionally, other bioactive molecules are being explored for attachment to the system in hopes of building a modular drug delivery system.

4. Conclusions

A novel functionalization of the outer surface of HNTs using the cancer-targeting molecule folic acid (FA) and the imaging agent fluorescein isothiocyanate (FITC) bound to the surface of the HNTs using the molecule 3-(2-aminoethyl) aminopropyltrimethoxysilane (DAS) was synthesized. We observed fewer DAS molecules bound to the HNT surface than has been reported in the literature by other studies and suggest this is due to incomplete washing methods used in these studies. Cytotoxicity studies indicated that bHNTs were not cytotoxic until CT26 cells were exposed to bHNT concentrations greater than 150 μg/mL. Microscopic studies showed that bHNTs were taken up by CTH 26 cells at all concentrations. The modification of HNTs with folic acid imparts the desired ability to target tumor cells selectively. The addition of FITC offers a method for quantifying the effectiveness of the bi-functionalized HNTs ability to actively target tumor cells, deliver a payload of chemotherapeutics loaded within the HNT lumen, and provide imaging data on drug efficacy. Additionally, the use of covalently bound molecules to functionalize the HNTs alleviated the aggregation that limits the LBL-modified HNTs. This work offers an alternative to LBL functionalization of the outer HNT surface for drug delivery applications.

Supplementary Materials: Supplementary materials are available online at http://www.mdpi.com/2076-3417/8/2/281/s1.

Acknowledgments: The authors wish to acknowledge the Louisiana Governor's Biotechnology Initiative and the China Scholarship Council for providing funding support for this project.

Author Contributions: All authors contributed to the writing of the manuscript. William R. Grimes, Antwine W. McFarland, Jr. and Yangyang Luo conducted the experiments and analyses. David K. Mills conceived of the concept and assisted with the analyses.

Conflicts of Interest: The authors have no conflicts of interest.

References

1. Yang, X.D.; Liu, H.; Zhai, G. Advanced nanocarriers based on heparin and its derivatives for cancer management. *Biomacromolecules* **2014**, *16*, 423–436. [CrossRef] [PubMed]
2. Wang, S.K.; Lee, Y.K.; Hah, H.J.; Ethirajan, M.; Pandey, R.K.; Kopelman, R. Multifunctional biodegradable polyacrylamide nanocarriers for cancer theranostics—A "see and treat" strategy. *ACS Nano* **2012**, *6*, 6843–6851. [CrossRef] [PubMed]
3. Deng, Z.J.; Morton, S.W.; Ben-Akiva, E.; Dreaden, E.C.; Shopswitz, K.E.; Hammond, P.T. Layer-by-layer nanoparticles for systemic codelivery of an anticancer drug and siRNA for potential triple-negative breast cancer treatment. *ACS Nano* **2013**, *7*, 9571–9584. [CrossRef] [PubMed]

4. Dreaden, E.C.; Morton, S.W.; Shopsowitz, K.E.; Choi, J.-H.; Deng, Z.J.; Cho, N.-J.; Hammond, P.T. Bimodal tumor-targeting from microenvironment responsive hyaluronan layer-by-layer (LbL) nanoparticles. *ACS Nano* **2014**, *8*, 8374–8382. [CrossRef] [PubMed]
5. Weissig, V.P.; Murdock, N. Nanopharmaceuticals (part I): Products on the market. *Int. J. Nanomed.* **2014**, *9*, 4357–4373. [CrossRef] [PubMed]
6. Green, M.R.; Manikhas, G.M.; Orlov, S.V.; Afanasyev, B.V.; Makhson, A.M.; Bhar, P.; Hawkins, M.J. Abraxane, a novel cremophor-free, albumin-bound particle form of paclitaxel for the treatment of advanced non-small-cell lung cancer. *Ann. Oncol.* **2006**, *17*, 1263–1268. [CrossRef] [PubMed]
7. Dai, L.Z.; Li, Q.; Shen, X.; Mu, C.; Cai, K. Dendrimerlike mesopourous silica nanoparticles as pH-responsive nanocontainers for targeted drug delivery and bioimaging. *ACS Appl. Mater. Interfaces* **2015**, *7*, 7357–7372. [CrossRef] [PubMed]
8. Surapaneni, M.S.D.; Das, S.K.; Das, N.G. Designing paclitaxel drug delivery systems aimed at improved patient outcomes: Current status and challenges. *SRN Pharmacol.* **2012**, *2012*, 623139. [CrossRef] [PubMed]
9. Yu, M.; Zheng, J. Clearance pathways and tumor targeting of imaging nanoparticles. *ACS Nano* **2015**, *9*, 6655–6674. [CrossRef] [PubMed]
10. Yu, M.K.; Park, J.; Jon, S. Targeting strategies for multifunctional nanoparticles in cancer imaging and therapy. *Theranostics* **2012**, *2*, 3–44. [CrossRef] [PubMed]
11. Luk, B.T.; Zhang, L. Current advances in polymer-based nanotheranostics for cancer treatment and Diagnosis. *ACS Appl. Mater. Interfaces* **2014**, *6*, 21859–21873. [CrossRef] [PubMed]
12. Bharali, D.J.; Yalcin, M.; Darwish, N.H.; Debreli Coskun, M.; Keating, K.A.; Lin, H.Y.; Davis, P.J.; Mousa, S.A. Targeted delivery of paclitaxel and doxorubicin to cancer xenografts via the nanoparticle of nano-diamino-tetrac. *Int. J. Nanomed.* **2017**, *12*, 1305–1315.
13. Shimizu, T.; Tolcher, A.W.; Papadopoulos, K.P.; Beeram, M.; Rasco, D.W.; Smith, L.S.; Gunn, S.; Smetzer, L.; Mays, T.A.; Kaiser, B.; et al. The clinical effect of the dual-targeting strategy involving PI3K/AKT/mTOR and RAS/MEK/ERK pathways in patients with advanced cancer. *Clin. Cancer Res.* **2012**, *18*, 2316–2325. [CrossRef] [PubMed]
14. Slowing, I.T.; Terywin, B.G.; Lin, S.Y. Effect of surface functionalization of MCM-41-type mesoporous silica nanoparticles on the endocytosis by human cancer cells. *J. Am. Chem. Soc.* **2006**, *128*, 14792–14793. [CrossRef] [PubMed]
15. Shchukin, D.G.; Mohwald, H. Surface-engineered nanocontainers for entrapment of corrosion inhibitors. *Adv. Funct. Mater.* **2007**, *17*, 1451–1458. [CrossRef]
16. Du, M.; Guo, B.; Liu, M.; Jia, D. Thermal decomposition and oxidation ageing behaviour of polypropylene/halloysite nanotube nanocomposites. *Polym. Polym. Compos.* **2007**, *15*, 321–328.
17. Ravtani, D.; Agrawal, Y.K. Multifarious applications of halloysite nanotubes: A review. *Rev. Adv. Mater. Sci.* **2012**, *30*, 282–295.
18. Gupta, N.; Lin, T.C.; Shapiro, M. Clay-epoxy nanocomposites: Processing and properties. *JOM* **2007**, *59*, 61–65. [CrossRef]
19. Yang, Y.; Chen, Y.; Leng, F.; Huang, L.; Wang, Z.; Tian, W. Recent advances on surface modification of halloysite nanotubes for multifunctional applications. *Appl. Sci.* **2017**, *7*, 1215. [CrossRef]
20. Sun, L.; Boyer, C.B.; Grimes, R.; Mills, D.K. Drug coated clay nanoparticles for delivery of chemotherapeutics. *Curr. Nanosci.* **2016**, *12*, 207–214. [CrossRef]
21. Lvov, Y.; Wang, W.; Zhang, L.; Fakhrullin, R. Halloysite clay nanotubes for loading and sustained release of functional compounds. *Adv. Mater.* **2016**, *28*, 1227–1250.
22. Patel, S.; Jammaladaka, U.; Sun, L.; Tappa, K.; Mills, D.K. Sustained release of antibacterial agents from doped halloysite nanotubes. *Bioengineering* **2016**, *3*, 1. [CrossRef] [PubMed]
23. Wei, W.; Abdullayev, E.; Hollister, A.; Mills, D.K.; Lvov, Y.M. Clay nanotube/poly(methyl methacrylate) bone cement composites with sustained antibiotic release. *Macromol. Mater. Eng.* **2012**, *297*, 645–653. [CrossRef]
24. Vergaro, V.; Abdullayev, E.; Lvov, Y.M.; Zeitoun, A.; Cingolani, R.; Rinaldi, R.; Leporatti, S. Cytocompatibility and uptake of halloysite clay nanotubes. *Biomacromolecules* **2010**, *11*, 820–826. [CrossRef] [PubMed]
25. Kryuchkova, M.; Danilushkina, A.; Lvov, Y.; Fakhrullin, R. Evaluation of toxicity of nanoclays and graphene oxide in vivo: A Paramecium caudatum study. *Environ. Sci. Nano* **2016**, *3*, 442–452. [CrossRef]
26. Nicholson, J.C.; Weisman, J.A.; Boyer, C.G.; Wilson, C.J.; Mills, D.K. Dry sintered metal coating of halloysite nanotubes. *Appl. Sci.* **2012**, *6*, 265–275. [CrossRef]

27. Cervini-Silva, J.; Nieto-Camacho, A.; Ramírez-Apan, M.T. The anti-inflammatory properties of different naturally-occurring halloysites. In *Natural Mineral Nanotubes: Properties and Application*; Pasbakhsh, P., Churchman, C.J., Eds.; Apple Academic Press: Oakville, ON, Canada; Waretown, NJ, USA, 2015; Chapter 24; pp. 449–460.
28. Wu, W.; Cao, X.; Luo, J.; He, G.; Zhang, Y. Morphology, thermal, and mechanical properties of poly(butylene succinate) reinforced with halloysite nanotube. *Polym. Compos.* **2014**, *35*, 847–855. [CrossRef]
29. Arat, R.; Uyanik, N. Surface modification of nanoclays with co-polymers. *Nat. Res.* **2017**, *8*, 159–171. [CrossRef]
30. Joo, Y.; Jeon, Y.; Lee, S.U.; Sohn, D. Aggregation and stabilization of carboxylic acid functionalized halloysite nanotubes (HNT-COOH). *J. Phys. Chem. C* **2012**, *116*, 18230–18235. [CrossRef]
31. Du, M.; Guo, B.; Jia, D. Thermal stability and flame retardant effects of halloysite nanotubes on poly(propylene). *Eur. Polym. J.* **2006**, *42*, 1362–1369. [CrossRef]
32. Carli, L.N.; Daitx, T.S.; Soares, G.; Crespo, J.S.; Mauler, R.S. PHBV nanocomposites based on organomodified montmorillonite and halloysite: The effect of clay type on themorphology and thermal and mechanical properties. *Compos. Part A* **2011**, *42*, 1601–1608. [CrossRef]
33. Liu, M.; Jia, Z.; Jia, D.; Zhou, C. Recent advance in research on halloysite nanotubes-polymer nanocomposite. *Prog. Polym. Sci.* **2014**, *39*, 1498–1525. [CrossRef]
34. Rooj, S.; Das, A.; Thakur, V.; Mahaling, R.N.; Bhowmick, A.K.; Heinrich, G. Preparation and properties of natural nanocomposites based on natural rubber and naturally occurring halloysite nanotubes. *Mater. Des.* **2010**, *31*, 2151–2156. [CrossRef]
35. Prashantha, K.; Lacrampe, M.F.; Krawczak, P. Processing and characterization of halloysite nanotubes filled polypropylene nanocomposites based on masterbatch route: Effect of halloysite treatment on structural and mechanical properties. *Express Polym. Lett.* **2011**, *5*, 295–307. [CrossRef]
36. Massaro, M.; Lazzara, G.; Milioto, S.; Noto, R.; Riela, S. Covalently modified halloysite clay nanotubes: Synthesis, properties, biological and medical applications. *J. Mater. Chem. B* **2017**, *5*, 2867–2882. [CrossRef]
37. Yah, W.O.; Takahara, A.; Lvov, Y. Selective modification of halloysite lumen with octadecylphosphonic acid: New Iinorganic tubular micelle. *J. Am. Chem. Soc.* **2012**, *134*, 1853–1859. [CrossRef] [PubMed]
38. Vigneron, N. Human tumor antigens and cancer immunotherapy. *BioMed Res. Int.* **2015**, *2015*, 948501. [CrossRef] [PubMed]
39. Wang, S.; Low, P.S. Folate-mediated targeting of antineoplastic drugs, imaging agents, and nucleic acids to cancer cells. *J. Control. Release* **1998**, *53*, 39–48. [CrossRef]
40. Sudimack, J.; Lee, R.J. Targeted drug delivery via the folate receptor. *Adv. Drug Deliv. Rev.* **2000**, *41*, 147–162. [CrossRef]
41. Qiao, J.; Mu, X.; Qi, L.; Deng, J.; Mao, L. Folic acid-functionalized fluorescent gold nanoclusters with polymers as linkers for cancer cell imaging. *Chem. Commun.* **2013**, *49*, 8030–8032. [CrossRef] [PubMed]
42. Yuan, P.; Southern, P.D.; Liu, Z.; Green, M.E.R.; Hook, J.M.; Antill, S.J.; Kepert, C.J. Functionalization of halloysite clay nanotubes by grafting with γ-aminopropyltriethoxysilane. *J. Phys. Chem. C* **2009**, *112*, 15742–15751. [CrossRef]
43. Zhang, H.; Ren, T.; Han, L.; Wu, Y.; Song, H.; Bai, L.; Ba, X. Selective modification of halloysite nanotubes with 1-pyrenylboronic acid: A novel fluorescence probe with highly selective and sensitive response to hyperoxide. *ACS Appl. Mater. Interfaces* **2015**, *7*, 23805–23811. [CrossRef] [PubMed]
44. Barrientos-Ramirez, S.; Ramires, G.M.; Ramos-Fernandez, E.V.; Sepulveda-Escribano, A.; Pastor-Blas, M.M.; Gonzalex-Montiel, A. Surface modification of natural halloysite clay nanotubes with aminosilanes. Application as catalyst supports in the atom transfer dadical polymerization of methyl methacrylate. *Appl. Catal. A Gen.* **2011**, *406*, 22–33. [CrossRef]
45. Andreia, F.; Peixoto, A.C.F.; Pereira, C.; Pires, J.; Freire, C. Physiochemical characterization of organosilylated halloysite clay nanotubes. *Microporous Mesoporous Mater.* **2016**, *219*, 145–154.
46. Nalinkanth, G.; Veerabadran, D.M.; Torchilin, V.; Price, R.R.; Lvov, Y. Organized shells on clay nanotubes for controlled release of macromolecules. *Macromol. J.* **2008**, *9*, 99–103.
47. Jin, Y.; Yendluri, R.; Chen, B.; Wang, J.; Lvov, Y. Composite microparticles of halloysite clay nanotubes bound by calcium carbonate. *J. Colloid Interface Sci.* **2016**, *466*, 254–260. [CrossRef] [PubMed]

48. Ahmed, F.R.; Shoaib, M.H.; Azhar, M.; Um, S.H.; Yousuf, R.I.; Hashmi, S.; Dar, A. In vitro assessment of cytotoxicity of halloysite nanotubes against HepG2, HCT116 and human peripheral blood lymphocytes. *Colloids Surf. B* **2015**, *135*, 50–55. [CrossRef] [PubMed]
49. Zhang, Y.; Gao, R.; Liu, M.; Yan, C.; Shan, A. Adsorption of modified halloysite nanotubes in vitro and the protective effect in rats exposed to zearalenone. *Arch. Anim. Nutr.* **2014**, *68*, 320–335. [CrossRef] [PubMed]
50. Bellani, L.; Giorgetti, S.; Riela, G.; Lazzara, A.; Scialabba, M.; Massaro, M. Ecotoxicity of halloysite nanotube—Supported palladium nanoparticles in *Raphanus sativus* L. *Environ. Toxicol. Chem.* **2016**, *35*, 2503–2510. [CrossRef] [PubMed]
51. Fakhrullina, G.I.; Akhatova, F.S.; Lvov, Y.; Fakhrullin, R.F. Toxicity of halloysite clay nanotubes in vivo: A Caenorhabditis elegans study. *Environ. Sci. Nano* **2015**, *2*, 54–59. [CrossRef]
52. Lvov, Y.M.; DeVillers, M.M.; Fakhrullin, R.F. The application of halloysite tubule nanoclay in drug delivery. *Expert Opin. Drug Deliv.* **2016**, *13*, 977–986. [CrossRef] [PubMed]
53. Panariti, A.; Miserocchi, G.; Rivolta, I. The effect of nanoparticle uptake on cellular behavior: Disrupting or enabling functions? *Nanotechnol. Sci. Appl.* **2012**, *5*, 87–100. [CrossRef] [PubMed]
54. Huy, Y.; Chen, J.; Li, X.; Huang, S.; Li, Y.; Xu, J.; Zhong, S. Multifunctional halloysite nanotubes for targeted delivery and controlled release of doxorubicin in vitro and in-vivo studies. *Nanotechnology* **2017**, *28*, 375101. [CrossRef] [PubMed]
55. Leporatti, S. Halloysite clay nanotubes as nano-bazookas for drug delivery. *Polym. Int.* **2017**, *66*, 1111–1118. [CrossRef]
56. Tully, J.; Yendluri, R.; Lvov, Y. Halloysite clay nanotubes for enzyme immobilization. *Biomacromolecules* **2015**, *17*, 615–621. [CrossRef] [PubMed]
57. Keeney, M.; Jiang, X.Y.; Yamane, M.; Lee, M.; Goodman, S.; Yang, F. Nanocoating for biomolecule delivery using layer-by-layer self-assembly. *J. Mater. Chem. B* **2017**, *3*, 8757–8770. [CrossRef] [PubMed]
58. Xue, Y.; Niu, M.; Gong, R.; Shi, D.; Chen, L.; Zhang, L.; Lvov, Y. Electrospun microfiber membranes embedded with drug-loaded clay nanotubes for sustained antimicrobial protection. *ACS Nano* **2015**, *9*, 1600–1612. [CrossRef] [PubMed]
59. Sánchez-Fernández, A.; Peña-Parás, L.; Vidaltamayo, R.; Cué-Sampedro, R.; Mendoza-Martínez, A.; Zomosa-Signoret, V.C.; Rivas-Estilla, A.M.; Riojas, P. Synthesization, Characterization, and in vitro Evaluation of Cytotoxicity of Biomaterials Based on Halloysite Nanotubes. *Materials* **2014**, *7*, 7770–7780. [CrossRef] [PubMed]
60. Bugatti, V.; Viscusi, G.; Naddeo, C.; Gorrasi, G. Nanocomposites based on PCL and halloysite nanotubes filled with lysozyme: Effect of draw ratio on the physical properties and release analysis. *Nanomaterials* **2017**, *7*, 213. [CrossRef] [PubMed]
61. Fan, L.; Zhang, J.; Wang, A. In situ generation of sodium alginate/hydroxyapatite/halloysite nanotubes nanocomposite hydrogel beads as drug-controlled release matrices. *J. Mater. Chem.* **2013**, *1*, 6261–6270. [CrossRef]